https://doi.org/10.5194/egusphere-2025-1108
Preprint. Discussion started: 22 April 2025

Evaluation of the Particulate Inorganic Carbon Export Efficiency in the Global Ocean

Jordan Toullec[1]

[1]Univ Brest, CNRS, IRD, Ifremer, UMR 6539, LEMAR, Plouzané, France,

Correspondence to: Jordan Toullec (toullec.jordan@gmail.com)

Abstract. The oceanic carbonate pump corresponds to the production and the sinking of particulate inorganic carbon (PIC) thanks to calcified planktonic organisms. In this study, the global PIC production from ocean colour satellite observations were combined with PIC flux observation from short-term sediment traps deployed during the last decades covering the global ocean. Coccolithophores are the main planktonic calcified group in the euphotic zone, with an important phenological blooming pattern and an important latitude dependant seasonal response. The present study highlights that the PIC production in the euphotic zone and the pelagic PIC flux varied among oceanic regions, depth and season. Based on a geographic matchup between the PIC flux from sediment traps and remote sensing climatology observation, correlation between net primary production (NPP) of particulate organic carbon (POC) in the euphotic zone and PIC flux is revealed. However, PIC production in the euphotic zone is not correlated with PIC flux at global scale, but only for delimited ocean basin such as in the North Atlantic and the Southern Ocean. Despite lower PIC production and PIC/POC ratios in the euphotic zone, temperate and subpolar areas are more efficient to export PIC compared to equatorial and subtropical areas (higher PIC production and PIC/POC ratios in the euphotic zone). The plankton phenology seems to be an important driver of PIC export efficiency (PE_{eff}) and PIC transfer efficiency (T_{eff}). Pelagic PIC dissolution is assumed to be responsible for the decrease in PE_{eff} and T_{eff}. In a context of climate change, any modification of plankton network community as well as modification PIC T_{eff} is expected to have consequences on surface alkalinity balance and CO_2 exchange between ocean and atmosphere. This study suggests that the 'packaging factor' corresponding to the vehicle of the biological carbon pump (marine snow aggregates, fecal pellets) and the plankton network (e.g. zooplankton community, microbial loop) may affect the PIC export efficiency and the PIC transfer efficiency.

1. Introduction

Through gravitational settling, the biological carbon pump (BCP) transports photosynthetically fixed CO_2 into the deep ocean for decades to centuries to come. Without the BCP, atmospheric CO_2 concentration would be twice as important (Passow and Carlson, 2012). Phytoplankton, due to photosynthesis, uptake CO_2 from the atmosphere to produce particulate organic carbon (POC). In other hand, calcified phytoplankton (such as coccolithophores), produce both POC and inorganic carbon (particulate inorganic carbon, PIC), often referred as calcium carbonate ($CaCO_3$), which releases CO_2 during the process of calcification, this is the counter pump effect (equation 1).

$$Ca^{2+} + 2HCO_3^- \rightarrow CaCO_3 + CO_2 + H_2O \qquad (1)$$

Even though calcification contributes to the release of CO_2, $CaCO_3$ is composed of carbon, and therefore all planktonic calcified organisms (such as coccolithophores, foraminifera and pteropods) transport also POC to deep waters through gravitational settling. Field observation of particulate sinking flux (PIC and POC) have been made over many decades to better understand the BCP. To estimate a particle flux, the sediment traps and Thorium-234 activity (^{234}Th activity) were the most widespread techniques to quantitatively estimate a sinking flux, both in terms of time and geography (Savoye et aal., 2006).

Coccolithophores contribute to 70-90% of PIC production in the North Pacific Ocean when the period is optimal (Ziveri et al., 2023) and are generally considered dominant at global scale (Knecht et al., 2023). In the global ocean, coccolithophores annually uptake more carbon in high-light, stratified, and low-nutrient surface waters (Balch et al., 2011; Krumhardt et al., 2017). The total annual $CaCO_3$ production by planktonic organisms is characterised by a high uncertainty, with a range of 0.7–4.7 Pg C y^{-1} (Berelson et al., 2007; Buitenhuis et al., 2019; Lee, 2001; Milliman et al., 1999). A large proportion of these $CaCO_3$ produced in the euphotic zone is dissolved within the first 300m of the ocean (Sulpis et al., 2021, Feely et al., 2002; Milliman et al., 1999), thereby increasing ocean alkalinity and CO_2 uptake (Sarmiento, 2013). This shallow dissolution is not yet clearly explained but considered to be associated to biological and ecological mechanisms (zooplankton and procaryotes mediated dissolution). The sedimentation of calcifying organisms constitutes an export flux of $CaCO_3$ with estimated range of 0.4–1.8 Pg C y^{-1} (Berelson et al., 2007).

At a global scale, particle export efficiency (PE_{eff}, corresponding to the POC sinking flux in the euphotic layer/ POC production) is higher at high latitudes and lower at low latitudes (Fig. 1, Henson et al., 2012). The Transfer efficiency (T_{eff}, corresponding to the proportion of primary production that is exported below the euphotic layer) is lower at high latitudes and higher at low latitudes (Fig. 1, Henson et al., 2012). It has been established that T_{eff} is not correlated with $CaCO_3$ export flux (Henson et al., 2012), but evidence from sediment trap collection suggests that coccoliths and coccospheres are transported more efficiently to depth when incorporated into fecal pellets or marine snow aggregates (Honjo, 1976; Pilskaln and Honjo, 1987). $CaCO_3$ incorporation into aggregates and fecal pellets support the idea that high PE_{eff} could be coupled with high $CaCO_3$ flux. Indeed, the incorporation of biominerals (such as $CaCO_3$ and biogenic silica) induces a ballast effect (excess of density) on marine snow sinking velocity (Iversen and Ploug, 2010; Laurenceau-Cornec et al., 2020) and hence expected to boost the BCP.

Seasonal influence is an important aspect of the T_{eff} of carbon to the deep sea and could be attributed to the greater lability of organic matter exported during phytoplankton blooms. In general, high latitudes are opal-productive regions (diatoms blooms) with high PE_{eff} and a higher fraction of the exported organic matter is remineralized before reaching bathypelagic depths (low T_{eff}). In low latitudes, which are $CaCO_3$-productive regions, a modelling study demonstrated that PE_{eff} is lower, but T_{eff} is expected to be higher (Fig. 1, Lima et al., 2014).

The ‘packaging factor’ theory suggests that $CaCO_3$-dominated ecosystems (subtropics and equatorial area) are associated with complex food web, and $CaCO_3$ would be more tightly packaged in fast-sinking fecal pellets. However, particle flux from seasonal, opal-dominated systems (Temperate and sub-Polar ecosystems) would be highly “degradable” formed aggregates, produced by the coagulation of senescent diatoms (Francois et al., 2002). This ‘packaging factor’ hence should be a strong driver of T_{eff} (Fig. 1).

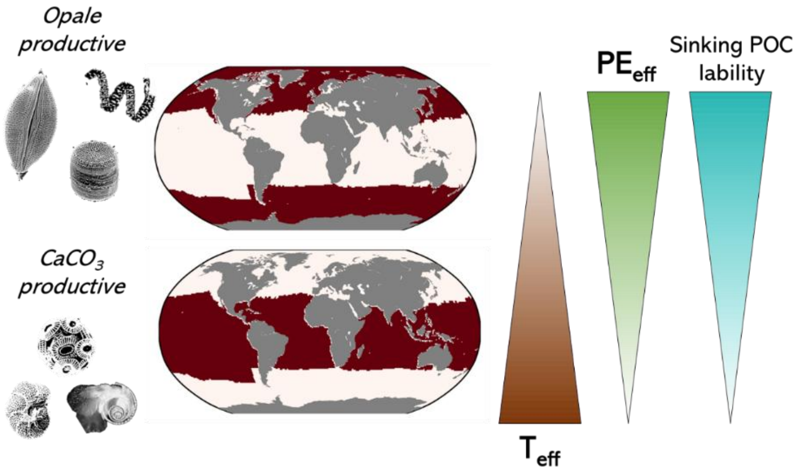

Figure 1: Biominerals produced by planktonic organisms according to the oceanic regions, and associated particles transfer dynamic.

The biogeographical approach is particularly appealing to understand the structures of plankton communities as well as biogeochemical processes according to the latitude and different ocean basins, also under climate change scenarios (Barton et al., 2013). Indeed, biogeographic patterns are common in macroecology (Kaneko et al., 2023; Thuiller et al., 2015), and PCB understanding (Clements et al., 2023; Ricour et al., 2023; Wang et al., 2023).

In this context, ocean colour data derived from satellite observation is valuable to estimate surface ocean processes over time. Satellite observations of coccolithophore blooms have been available since the emergence of remote sensing of ocean colour techniques (Holligan et al., 1993). Blooms of coccolithophores (e.g., *Emiliania huxleyi*) can result in patches of high reflectivity at the surface of the ocean and are associated with unique optical properties (Balch et al., 1996, 2005; Balch and Mitchell, 2023) that can be used to estimate PIC concentration and production at the global scale and production rate (Hopkins & Balch, 2018; Hopkins et al., 2019). There remains a gap between the amount of photosynthetically produced organic carbon, and it transferred fraction to the deep. Nowadays, heterotrophic respiration in sinking aggregates is considered to dissolve $CaCO_3$ particles in the upper ocean. In the deep ocean, dissolution of $CaCO_3$ is primarily driven by conventional thermodynamics of $CaCO_3$ solubility with reduced fluxes of $CaCO_3$ burial to marine sediments. Without upper ocean $CaCO_3$ dissolution, the ocean output 20% more CO_2 to the atmosphere through the low-latitude upwelling regions (kwon et al., 2024).

Understanding how the surface processes control the export of POC and PIC is still an ongoing challenge in the biogeochemical oceanographic community. In addition, processes of PIC production, sinking flux and dissolution are crucial to understand ocean alkalinity balance, which holds the uptake of atmospheric carbon and acidification in surface waters (Planchat et al., 2023). This study examines the variability in surface PIC production and PIC flux. A compilation of existing data sources (PIC flux from sediment traps) and ocean colour data obtained from remote sensing, geographically covering the open ocean at different seasonal scales is compared and discussed. The objective of this study is to address the following questions: What environmental factors can explain the PIC export efficiency (PIC E_{eff}) and the PIC transfer efficiency (PIC T_{eff}) at the global scale?

2. Materials and Methods

2.1. PIC production remote sensing-based modelling

PIC production at a global scale was modelled using satellite ocean colour measurements (see Hopkins and Balch, 2018 and reference inhere for more details), coupled with physiological constant associated with *Emiliania huxleyi*, which is the most cosmopolitan coccolithophore and extensive blooms former (Holligan et al., 1993) across the majority of the world's oceans (Tyrrell and Merico, 2004).

2.1.1. Calcification model

The model proposed by Hopkins et Balch (2018) was applied to estimate the calcification rate in the euphotic zone (expressed as EZ PIC production). The model of coccolithophores calcification rate is a function of PIC concentration, growth rate, irradiance, and depth (Equation 2):

$$PIC\ production = f[PIC, \mu, h(surf), g(Z_{eu})] \qquad (2)$$

In this model, general assumptions are made, such as the PIC production is proportional to the coccolithophore growth rate. The coccolithophore growth rate is a function of temperature and irradiance (parameters established on *Emiliania huxleyi* culture). The calcification rate decreases as a function of light availability through the water column (Hopkins and Balch, 2018). The model generalizes the euphotic zone integrated PIC production rate (g C m^{-2} d^{-1}) (Equation 3):

$$EZ\ PIC\ production = PIC\ concentration \times \mu \times h\left(I_{surf}\right) \times g(Z_{eu}) \qquad (3)$$

Where μ is a temperature-derived growth rate, $h(I_{surf})$ is a growth limiting irradiance function, and $g(Z_{eu})$ is a depth dependency function (see Hopkins and Balch, 2018 and reference inhere for more details). All the satellite products used in the model are described in the following section.

2.1.2. PIC and POC standing stock

Surface PIC and POC satellite-based concentrations were depth integrated to 100 m to using empirical relationships based on *in situ* measurements across the Atlantic Ocean (Balch et al., 2018):

$$PIC_{100m} = 40.555 \times PIC_{surface}{}^{0.560} \qquad (4)$$

$$POC_{100m} = 164.376 \times POC_{surface}{}^{0.617} \qquad (5)$$

2.1.3. Satellite products collection

The computation was performed with 1° by 1° grid average monthly data (from September 1997 to October 2023) from different sensors merged (Table 1). The satellite data used in this study (PIC concentration, PAR and Kd_{490nm}) were downloaded from the Globcolour website (https://www.globcolour.info/). The Sea surface temperatures were obtained from NASA Ocean Color website (https://oceancolor.gsfc.nasa.gov/) and the COPERNICUS marine service website (https://marine.copernicus.eu/fr). The following product (Table 1) were used in determining the PIC production rate (g C m^{-2} d^{-1}): The monthly surface PIC concentration (mol C m^{-3}); The monthly SST (Sea Surface Temperature in °C) for the determination of *Emiliania huxleyi* growth rate; The monthly photosynthetic available radiation (PAR; mol photons m^{-2} d^{-1})

for the growth rate limiting irradiance; The monthly Kd_{490nm} (Light diffuse attenuation coefficient at 490 nm; m^{-1}) used for the determination of the euphotic depth and depth-integrated calcification rate, see details of the methods below. Euphotic zone integrated Primary Production (mg C m^{-2} d^{-1}) was obtained from COPERNICUS marine service website (https://marine.copernicus.eu/fr; DOI:10.48670/moi-00281), the different variables were obtained from multi-sensors products based on SeaWiFS, MERIS, MODIS-A, MODIS-T, VIIRS-SNPP & JPPS1, OLCI-S3A & S3B). The primary production algorithm was developed by Antoine and Morel (1996).

Table 1: Satellite products merged in the analyses. AV = Simple average method; AVW = Weighted average method; SWF = Sea-Viewing Wide Field of View Sensor (SeaWiFS); MOD = Moderate Resolution Imaging Spectrometer (MODIS); VIR = Visible Infrared Imaging Radiometer Suite (VIIRS); MER = Medium Resolution Imaging Spectrometer (MERIS); OLA = Ocean and Land Color Instruments (Sentinel-3A); Vj1 = VIIRS aboard JPSS-1 (Joint Polar Satellite System); OLB = Ocean and Land Color Instruments (Sentinel-3B).

Periods	**Monthly PIC concentration**	**Monthly SST**	**Monthly PAR**	**Monthly Kd_{490nm}**
	mol C m^{-3}	°C	mol photons m^{-2} d^{-1}	m^{-1}
Sept 1997- April 2002	AV-SWF	ESA SST CCI and C3S and C3S reprocessed SST	AV-SWF	AV-SWF
May 2002- June 2002	AV-SWF	ESA SST CCI and C3S reprocessed SST	AV-SWF	AVW-MERSWF
July - 2002 - Dec 2010	AVW-MODSWF	MODIS	AVW-MODSWF	AVW-MERMODSWF
Jan- 2011 - Jan 2012	AV-MOD	MODIS	AV-MOD	AVW-MERMOD
Febr - 2012 - Apr 2012	AVW-MODVIR	MODIS	AVW-MODVIR	AVW-MERMODVIR
May - 2012 - Apr 2016	AVW-MODVIR	MODIS	AVW-MODVIR	AVW-MODVIR
May 2016 - Nov 2017	AVW-MODVIR	MODIS	AVW-MODVIR	AVW-MODVIR
Dec 2017 - Mar 2019	AVW-MODVIR	MODIS	AVW-MODVIR	AVW-MODVIR
Apr 2019 - Oct 2023	AVW-MODVIR	MODIS	AVW-MODVIR	AVW-MODVIR

2.2. PIC flux

2.2.1. Sediment trap data collection

PIC flux from sediment trap data was obtained from public repositories and published data (https://www.pangaea.de/, see Table 2; Fig. 2).

Table 2: PIC flux dataset compilation.

Data sets	**Reference**
https://doi.org/10.1594/PANGAEA.855600	Mouw et al., 2016
https://doi.org/10.1594/PANGAEA.807946	Torres Valdés et al., 2014
Supplementary material: https://agupubs.onlinelary.wiley.com/doi/10.1002/2014GL061678	Le Moigne et al., 2014
https://doi.org/10.1594/PANGAEA.934361	Fischer et al., 2016
https://doi.org/10.1594/PANGAEA.867116	
https://doi.org/10.1594/PANGAEA.863969	Romero et al., 2016
Table 2	Rosengard et al., 2015
Table 1	Neukermans et al., 2023

To ensure that the time scale of the PIC flux corresponds as closely as possible to the products derived from the satellites, analysis on a subset of sediment traps deployed 31 days or less (monthly), for a total of 6057 PIC flux observations (sediment traps deployed from 1983 to 2012) were performed. PIC flux observation was then aggregated into seven different layers of depth (0-100m, 100-500m, 500-1000m, 1000-2000m, 2000-3000m, 3000-4000m and > 4000m), as presented in Table 3. Analysis on monthly deployed sediment flux were matched with monthly remote-sensing climatology (see details in the following section). On the other hand, a possible bias associated with the interaction of hydrodynamics, the capture of zooplankton, organic particle remineralization, and PIC dissolution could happen for a longer time of deployment.

Table 3: Layer of the depth of the subset used in the analysis.

Depth layer	Number of PIC flux observation	Number of sediment traps (location according to 1° by 1° grid map)
0-100m	101	84
100-500m	996	62
500-1000m	1175	54
1000-2000m	1405	64
2000-3000m	730	64
3000-4000m	1077	35
> 4000m	573	28

A total of 262 sediment trap locations were used in the analysis. Note that the total of sediment traps for each layer of depth is equal to 388, due to the multiple depth deployment at the same geographic location. Moreover, multiple PIC flux observations can be attributed to the same sediment trap deployment (time series, e.g.: PAP, ALOHA station). As for EZ PIC production model output, the analysis and interpretation of observed PIC flux were applied to the open ocean only, excluding data obtained from a water column of less than 200 m depth.

2.2.2. Global data flux estimates

Total global EZ PIC production (Pg C yr^{-1}) was determined by multiplying integrated PIC production by the latitudinally varying area of each 1° by 1° pixel. The latitude variation pixel surface (m^2) was computed using equation 6:

$$Surface\ (m^2) = \left[\frac{40\ 075.017 \times cos\left(\frac{\pi}{180}(Latitude)\right)}{360} \times \frac{\frac{40\ 007.864}{2}}{180}\right] \times 10^6 \qquad (6)$$

Where the equatorial earth circumference = 40 075.017 km^2 and the meridional earth circumference = 40 007.864 km^2. The data downloaded were a matrix of 180 pixels of latitude by 360 pixels of longitude (based on cylindric projection).
The analysis and interpretation of the EZ PIC production model output were focus on the open ocean only, excluding data obtained from water columns of less than 200 m depth.

2.2.3. Biogeochemical regions

RECCAP2 biogeochemical regions (second REgional Carbon Cycle Assessment and Processes) aim to accurately assess land and ocean CO_2 sources and sinks through the efforts of hundreds of scientists around the globe (Hauck et al., 2023). The overall aim of RECCAP2 is to support the Global Carbon Project (https://www.globalcarbonproject.org/) and the stocktaking of greenhouse gases by providing a reliable scientific basis for the transport of carbon between land, ocean and atmosphere. RECCAP2 biogeochemical regions mask was used to aggregate data from sediment traps and remote sensing according to relevant geographical regions (Fig.2, Table S1).

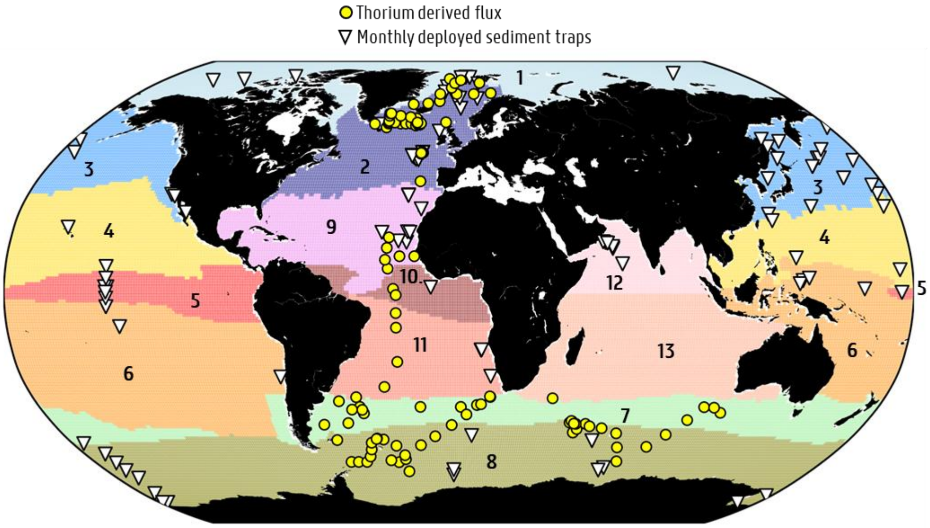

Figure 2: Location of sediment traps measuring PIC flux within 13 biogeochemical regions (RECCAP 2 regions). Region 1 = Arctic (Ar); 2 = North Atlantic (NA); 3 = North Pacific (NP); 4 = North Subtropics Pacific (NSTP); 5 = Equatorial Pacific (EP); 6 = South Subtropics Pacific (SSTP); 7 = Subantarctic (SAZ); 8 = Antarctic (AAZ); 9 = North Subtropics Atlantic (NSTA); 10 = Equatorial Atlantic (EA); 11 = South Subtropics Atlantic (SSTA); 12 = North Indian Ocean (NI) and 13 = South Indian Ocean (SI). The monthly deployed sediment traps are depicted by white triangles and Thorium-derived PIC flux is depicted by yellow dots.

54 tations were out of the RECCAP2 mask and then have been removed from the 6057 PIC flux observations subset.

2.2.4. Euphotic zone integrated satellite-derived production and deep PIC flux matchup

The majority of sediment trap deployment occurred before the launch of ocean colours observation from satellite, from 1983 to 2012 (SeaWiFS observation started in September 1997). 75.7% of PIC flux data used in the analysis (4588 observations over a total of 6057 observations) were collected before the satellite record. Hence, a match-up between the PIC flux data and EZ PIC production monthly climatology were performed (monthly mean from September 1997 to November 2023).
In the analysis, 7 different layers of depth were aggregated (0-100m, 100-500m, 500-1000m, 1000-2000m, 2000-3000m, 3000-4000m and > 4000m). Discrete observed PIC flux values obtained from sediment traps were aggregated over the depth layer of interest and matched geographically with the monthly climatology-modelled EZ PIC production and NPP on the 1°×1° grid. PIC flux values were therefore matched to the same 1° pixel and then associated to the same EZ PIC production. The monthly climatology average of EZ PIC production was established on a period from September 1997 to November 2023 on the 1°×1° grid map. Pearson’s correlation test was performed between the monthly climatology average of EZ PIC production and PIC flux values for the depth layers of interest. The process has been performed for the 13 RECCAP2 biogeochemical regions, covering the global ocean.
EZ PIC production values < 0.1 mg m^{-2} d^{-1} were removed from the dataset, to avoid values close to zero or detection limit, due to no covering of the satellite (e.g. winter months in the north hemisphere above 40°N).

3. Results

3.1. NPP, PIC production and residence time seasonality

At the global scale, annual EZ PIC production of 1.65 ± 0.36 Pg C y^{-1} was estimated (monthly mean ± σ, 1997-2023 annual mean), which is congruent with previous estimation based on the same calcification model (ca. 1.42 ± 1.69 Pg C y^{-1} in Hopkins and Balch, 2018). The difference in the estimation could be explained by the satellite product quality (resolution) and the number of months used in the model.

The most NPP annual productive areas are located along the continental margins, above 40°N and within equatorial upwelling ecosystems (Fig. 3a). In contrast to the NPP, the most PIC productive areas are located within subtropical gyres, and less productive within equatorial upwelling ecosystems (Fig. 3b). The seasonal variation of NPP and PIC production follows the phytoplanktonic bloom phenology, with higher seasonal variation above 40°N and below 40°S (Fig. 3c and d). It is noticeable that the PIC production seasonal bias amplitude is higher than NPP seasonal bias (Fig. 3c and d). Both residence time and amplitude variation are higher for PIC than for POC (Fig. 3e and f). The amplitude of spatial variation of POC residence time is lower than PIC residence time (Fig. 3e and f). The residence time is obtained by dividing the euphotic layer integrated standing stock (g m^{-2}) by the euphotic layer integrated production rate (g m^{-2} d^{-1}). POC residence time highest values reach 20 days in the Southern Ocean and over 20 days in arctic regions (Fig. 3e). However, PIC residence time values reach more than 30 days at high latitudes (the Southern Ocean and above 40°C). PIC residence time values over 10 days are also observed within equatorial upwelling (Indian Ocean and West Pacific equatorial).

https://doi.org/10.5194/egusphere-2025-1108
Preprint. Discussion started: 22 April 2025

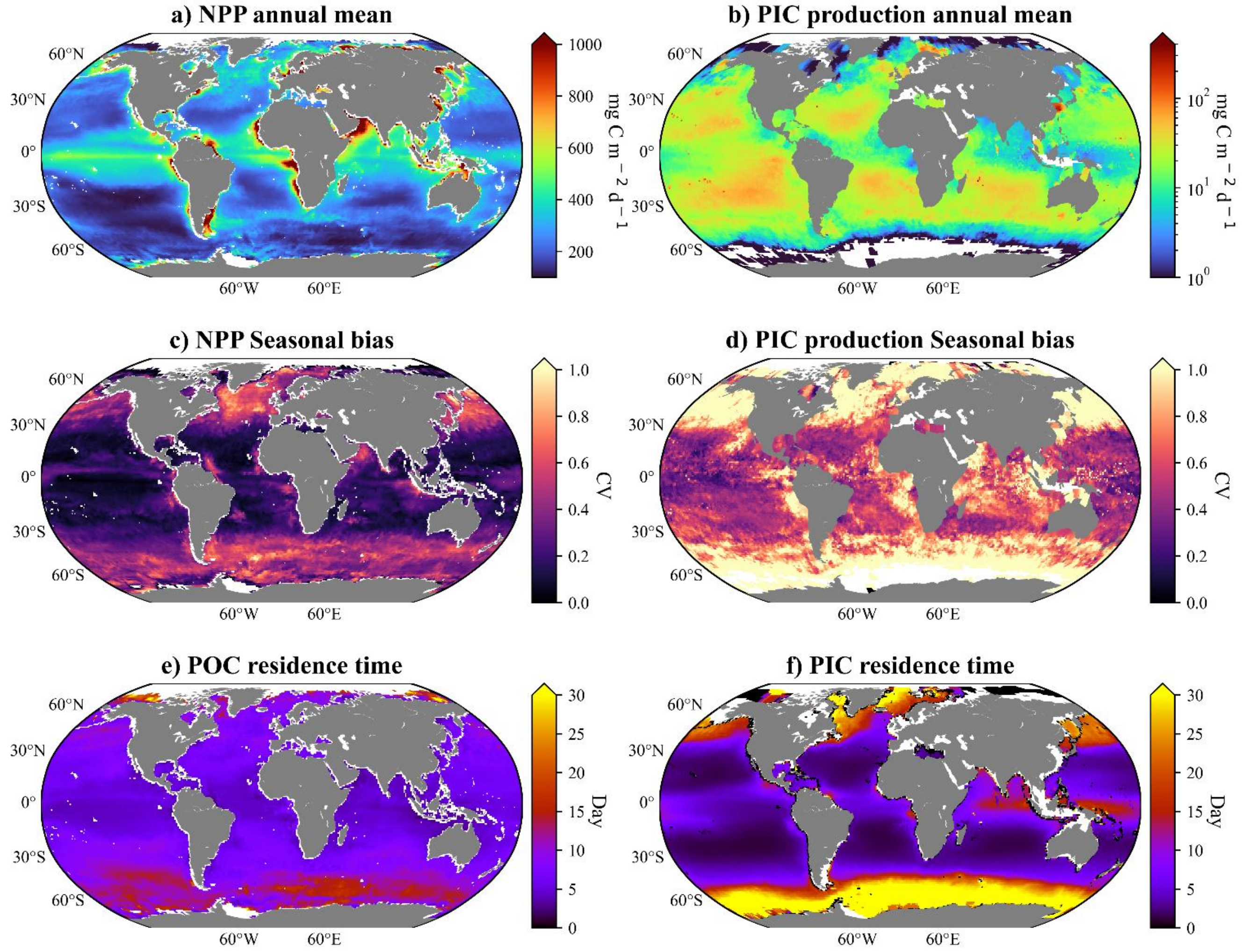

Figure 3: Global maps of (a) NPP annual mean (mg POC m^{-2} d^{-1}, 1997-2023 annual mean), (b) PIC production annual mean (mg PIC m^{-2} d^{-1}, 1998-2023 annual mean), (c) NPP seasonal bias expressed as coefficient of variation (σ/μ), (c) PIC production seasonal bias expressed as coefficient of variation (σ/μ), (e) POC residence time (day, 1997-2023 annual mean) and (f) PIC residence time (day, 1998-2023 annual mean).

3.2. PIC production, NPP and PIC flux

No significant correlation between log-transformed PIC flux and log-transformed NPP is observed between the surface and 100m depth (Fig. 4). On average, despite the Pearson's correlation coefficient R^2 are low (< 0.25), higher R^2 coefficients are observed when the PIC flux is correlated with NPP compared as compared to PIC production (Fig. 4). The deepest layer (>4000m) is characterised by higher correlation between PIC flux and PIC production than between PIC flux and NPP (respectively 0.104 and 0.089).

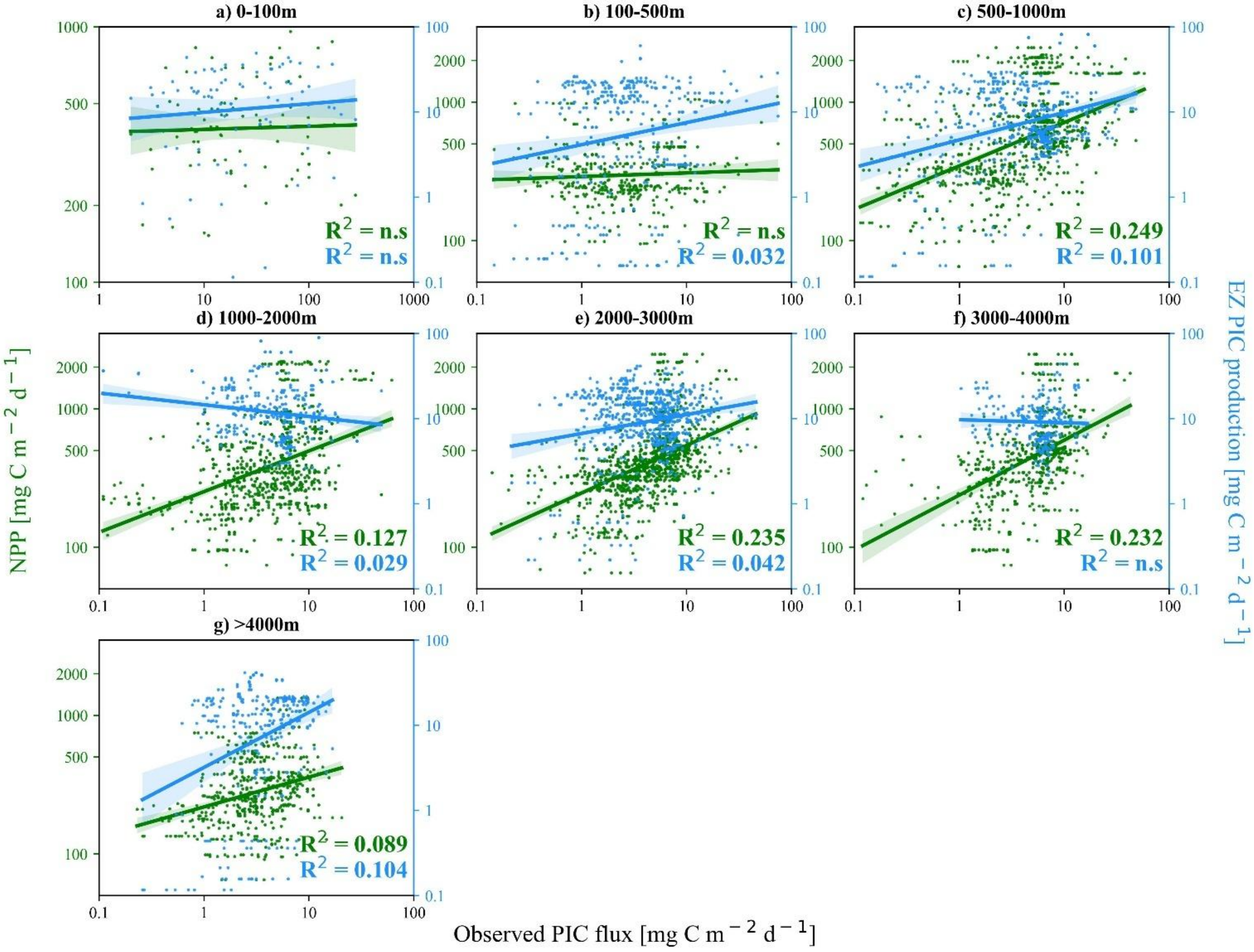

Figure 4: Matchup between observed sediment traps PIC flux (x-axis, mg PIC m^{-2} d^{-1}) and NPP (mg POC m^{-2} d^{-1}) in green, and satellite-derived PIC production (mg PIC m^{-2} d^{-1}) in blue (Hopkins et Balch, 2018 model). The different windows correspond to the different layers of depth.

3.3. Correlation between EZ PIC production and deep PIC flux

Most of the RECCAP2 biogeochemical regions have no observations of PIC flux or are insufficient to perform correlation in shallow waters (0-100m depth). PIC flux established in shallow waters (0-100m depth) in the North Atlantic was collected during the productive period (May, June, July and August), and does not reflect the EZ PIC production seasonal variation (a non-significant correlation between EZ PIC production and PIC flux has been established, see Table S2). At the global scale, the linear regression and correlation test between EZ PIC production and PIC flux are displayed for the 6 layers of depth (100-500m, 500-1000m, 1000-2000m, 2000-3000m, 3000-4000m and > 4000m) and regarding the RECCAP2 biogeochemical regions in the Fig. 5 (see Table S2, for the linear regression parameters).

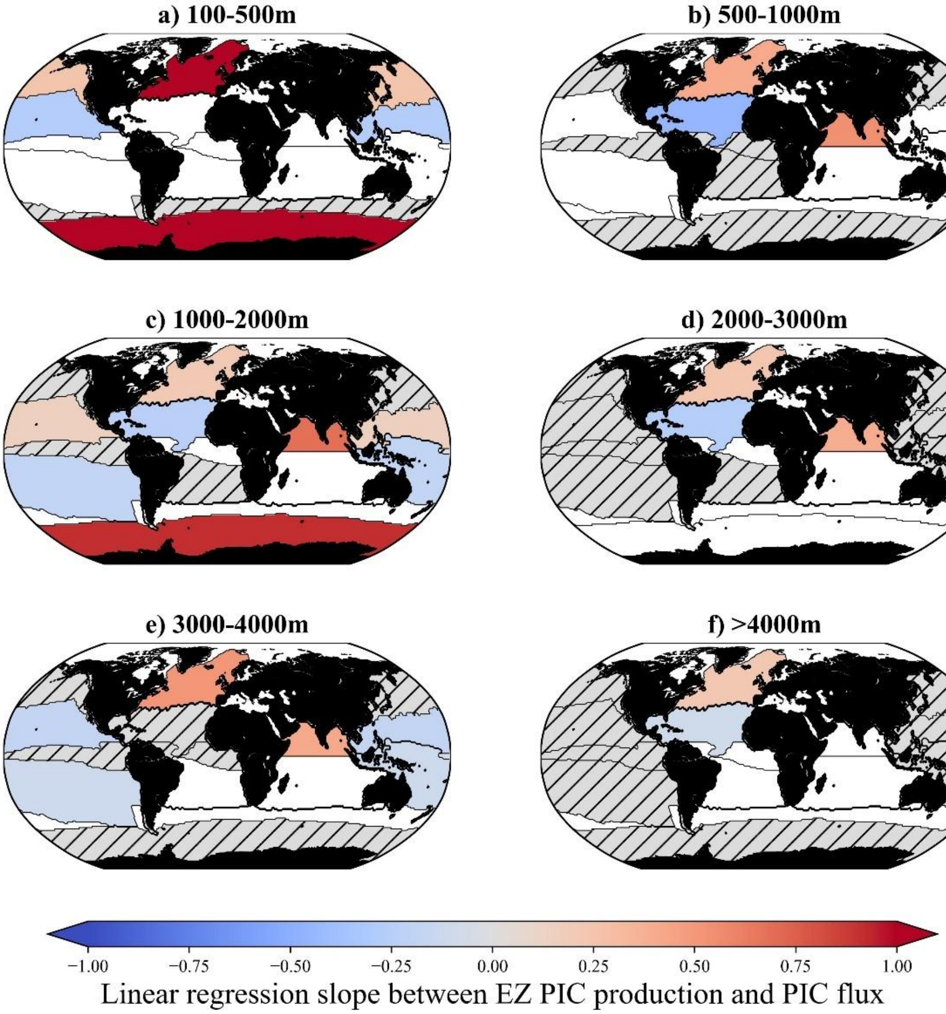

Figure 5: Map of linear regression slope between EZ PIC production and PIC flux according to the RECCAP2 regions and depth layers. Hatched grey areas correspond to regions and/or depths where the correlation coefficient is non-significant at a 95 % threshold ($p\text{-value} < 0.05$). White areas correspond to regions where no data are available.

The PIC export efficiency (PIC E_{eff}) corresponds to the PIC export flux divided by the EZ PIC production. A latitudinal variability trend could be overlapped to both NPP and PIC production SB (Fig. 6a). Regions above 40°, are characterized by higher PIC export efficiency (PIC E_{eff}) compared to subtropics and equatorial areas (Fig. 6a). The seasonality of NPP and PIC production can be overlapped with aggregates's contribution to the export (estimated by Nowicki et al., 2022), as shown in Fig. 6b. The contribution of fecal pellets to the export (estimated by Nowicki et al., 2022) increases continuously from 40° to the equator, while aggregates's contribution to the export decreases. The higher contribution of fecal pellets to the export coincides with low normalized PIC export efficiency (PIC E_{eff}) (Fig. 6b).

https://doi.org/10.5194/egusphere-2025-1108
Preprint. Discussion started: 22 April 2025

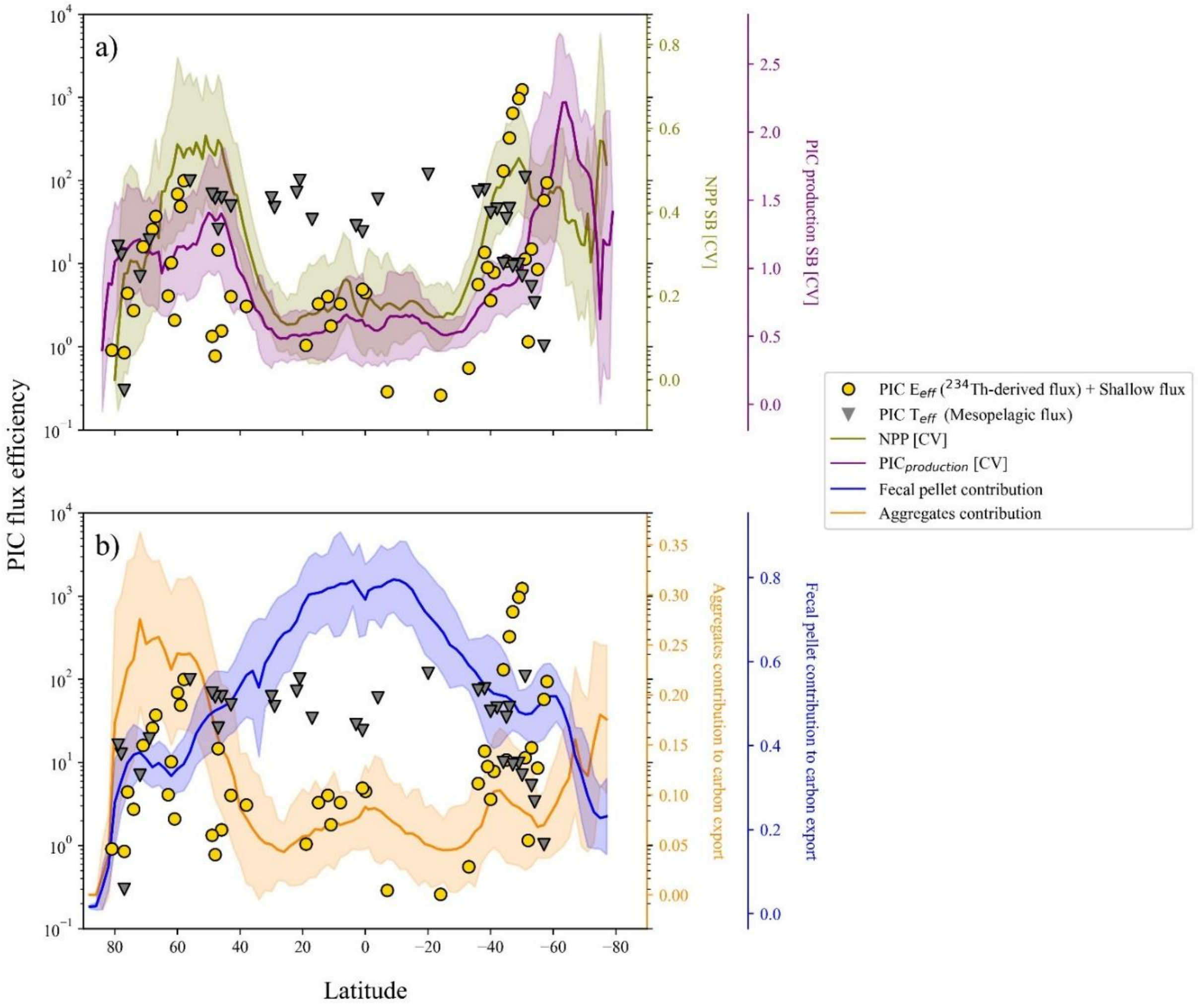

Figure 6: Depicted in the left y-axis: The yellow circles represent the latitudinal annual mean PIC Export efficiency (PIC E_{eff}) from shallow sediment traps (0-100m) and ^{234}Th-derived flux over the latitude (x-axis). The grey triangles represent the latitudinal mean PIC Transfert efficiency (PIC T_{eff}) from mesopelagic sediment traps (100-1000m). a) Annual PIC production seasonal bias (C.V) in purple and NPP seasonal bias (C.V) in green. b) Annual Fecal pellets contribution to the total carbon export (Nowicki et al., 2022) in blue and Annual aggregates contribution to the total carbon export (Nowicki et al., 2022) in orange.

4. Discussion

The fraction of phytoplankton exported production that is remineralized, is mainly influenced by ecosystem structure, which is related to the seasonal amplitude in NPP. Diatoms and coccolithophores are dominant in productive areas associated with high annual mean and amplitude of NPP, while nanoplankton/picoplankton are dominant in oligotrophic areas associated with low annual amplitude of NPP (Lima et al., 2014). The 'ballast effect hypothesis' induced by the inclusion of biominerals (calcite and biogenic silica) has been considered for a long time to boost the particle export efficiency (PE_{eff}), which corresponds to the proportion of primary production that is exported from the surface ocean. The PE_{eff} is commonly higher above 40°N and below 40°C (temperate oceanic regions), while the transfer efficiency (T_{eff}), which corresponds to the fraction of exported organic matter that reaches the deep ocean, is higher between 40°N and 40°S (subtropics), and follow the pattern than fecal pellet contribution to the export (Fig. 6). Despite a higher PIC production estimated by the model proposed by Hopkins et al., 2018, PIC transfer efficiency seems to be lower in subtropic regions compared to temperate regions.

4.1. Mesopelagic PIC flux & ballast effect hypothesis

The ballast hypothesis is derived from correlations between POC flux and mineral fluxes (opale and $CaCO_3$) in deep sediment traps (Klaas and Archer, 2002). However, it has been demonstrated that $CaCO_3$ export flux in the upper ocean is not correlated with the transfer efficiency (Henson et al., 2012). These points suggest that the association of $CaCO_3$ and POC does not decrease the degradation via a ballasting effect at mesopelagic depths. Indeed, Henson et al. (2012) concluded that ecosystem structure is the key factor controlling the efficiency of the biological carbon pump, rather than the ballast effect induced by $CaCO_3$. François et al. (2002) hypothesized the 'packaging factor' theory, explaining that high $CaCO_3$ productive systems (Subtropics) also contain organisms that produce singing fecal pellets capable of efficiently delivering organic carbon to deep waters (e.g model from Nowicki et al. 2022). In support of the ballast effect theory, Le Moigne et al. (2014) demonstrated that in the North Atlantic, 60% of the POC flux is associated with ballast biominerals (opal and $CaCO_3$), and about 40% in the Southern Ocean. In other regions (Subtropics and equatorial upwelling regions), the export flux is not associated with mineral ballasts. These statements highlight the great spatial variability of biomineral inclusion into sinking particles.

The results presented in this study demonstrates at the global scale that the EZ PIC production is not correlated with PIC flux in the upper ocean. However, considering distinct oceanic bioregions (RECCAP2), in the mesopelagic layer and deeper, significant correlations between EZ PIC production and deep PIC flux are observed in the North Atlantic and the Southern Ocean. These correlations are observed on every layer of depth and present the best R^2 coefficient (Table S2). North Indian Ocean regions (subtropical areas) are also characterized by PIC production positively correlated with deep PIC flux (Fig. 5). The hypothetic processes behind theses variability are discussed in the following part of this section, regarding the planktonic functional composition and the phenological dynamic.

4.2. Ocean pattern of PIC saturation depth

The Surface Ocean (0-500m) is oversaturated with carbonate (CO_3^{2-}), bicarbonate ions (HCO_3^-) and calcium carbonate ($CaCO_3$) that compose calcite coccoliths, foraminifera' tests and aragonite shells (also other minor marine pelagic organisms such as ostracods valves, Brandão et al., 2019). $CaCO_3$ solubility increases with depth (higher pressure and low temperature), while calcified plankton decreases with depth. As photosynthetic organisms, living coccolithophores are strictly located in the euphotic layer, whereas 62 % of all pteropods' biomass is located within the top 200 m, the remaining biomass (38 %) is distributed down to 2000 m (Bednaršek et al., 2012; Burridge et al., 2017). As a result, $CaCO_3$ saturation is considerably reduced with depth, the ocean then becomes undersaturated and dissolution can occur. The depth where the dissolution starts to increase considerably is called the lysocline. The Carbonate Compensation Depth (CCD) also called saturation depth is defined as the horizon depth where the $CaCO_3$ sinking flux equals the $CaCO_3$ dissolution rate. However, $CaCO_3$ dissolution kinetics are relatively slow (Berner and Morse, 1974), this is why $CaCO_3$ can be found below the lysocline and CCD, while it is packaged into fast sinking aggregates and fecal pellets.

4.3. Taxa contribution to global PIC stock and production

There is large uncertainty in total $CaCO_3$ production in the water column, with current estimates ranging between 0.7–4.7 Pg C yr^{-1} (Berelson et al., 2007; Buitenhuis et al., 2019; Lee, 2001). The relative contribution of coccolithophores, foraminifera and pteropods to global production is also a big source of uncertainty. Bednaršek et al., (2012), estimated that pteropods' global annual biomass production was 5 times higher than foraminifera, but 1.5 to 3 times lower than coccolithophores (based on Balch et al., 2007, Knecht et al., 2023). According to estimates based on mechanistic modelling studies, Gangstø et al. (2008), calculated a total net pteropods $CaCO_3$ production of 0.87 Pg C yr^{-1}, representing 20–42 % of the global $CaCO_3$ budget (Lebrato et al., 2010). Then Buitenhuis et al., (2019), still through mechanistic models, evaluated a global $CaCO_3$ production by pteropods of 4.2 Pg C yr^{-1} (89% of CaCO3 total production). Concerning the foraminifera, Schiebel (2002), estimated a variability in global foraminifera $CaCO_3$ production ranging from 0.036 to 0.065 Pg C y^{-1}, representing 2-4% of $CaCO_3$ total production (Lebrato et al., 2010). In the work of Buitenhuis et al., (2019), the global foraminifera $CaCO_3$ production was estimated to be 0.14 Pg C yr^{-1} (3% of $CaCO_3$ total production). However, the relative production rate of pteropods and foraminifera compared to coccolithophore at global scale is not evaluated in this study and remain uncertain. However, Ziveri et al. (2023) showed that coccolithophore represented ~90% of total $CaCO_3$ production in the North Pacific Ocean, while pteropods and foraminifera played a secondary role.

4.4. Mesopelagic PIC flux "biological gatekeeper"

The 'packaging factor' theory hypothesized by François et al. (2002), suggests that subtropics and equatorial areas ($CaCO_3$-dominated ecosystem, Fig. 1) are associated with fast sinking fecal pellets production and so high PIC export flux. Regarding the particles' dependant export output model of Nowicki et al. (2022) (Fig. 6), the relative contribution of fecal pellet to carbon export flux is higher in subtropics and equatorial areas, compared to aggregates contribution. However, PIC export flux and deeper flux in our dataset are globally lower in these regions (despite higher PIC production), which is the opposite of the idea that packaged $CaCO_3$ into the fecal pellet is protected from dissolution and induce a ballast effect. Regarding the Aggregate's contribution to carbon export flux (Fig. 6), opal-dominated systems (Temperate and sub-Polar ecosystems), are associated with high PIC flux, which is also in contradiction with the 'packaging theory' suggesting highly labile formed aggregates (susceptible to be easily disaggregated and remineralized).

This calcite loss in the upper ocean is generally attributed to biologically mediated dissolution and more specifically by zooplankton grazing or transport. Zooplankton and bacterial activities decrease with depth (Hernández-León et al., 2020), and intense zooplankton grazing and biologically mediated PIC dissolution should occur in the epipelagic and mesopelagic layer (Sulpis et al., 2021). However, once the $CaCO_3$ is packaged into aggregates or fecal pellets, it should be protected from surrounding seawater and associated dissolution process, regardless of the respective depths of calcite and aragonite saturation. In that way, packaged $CaCO_3$ into aggregates of fecal pellet that settle below the saturation depth should be protected from surrounding seawater. However, zooplankton grazing could also induce aggregate fragmentation in the epipelagic and mesopelagic layers, which could be responsible for the loss of PIC in shallow waters (Toullec et al., 2019 and references in there).

4.4.1. Process of biological-mediated PIC dissolution

In 2011, Bisset et al. observed that the heterotrophic bacteria colonising calcium carbonate particles (foraminifer and oyster shells) did not cause any apparent dissolution (Bissett et al., 2011). More recently, it has been shown that the increase in hydrostatic pressure with depth during the sedimentation of *Emiliania huxleyi* aggregates does not seem to modify the dissolution of calcite or the remineralisation of POC (Tamburini et al., 2021). However, the community of bacteria colonising the aggregates, as well as the consumption of O_2, was strongly reduced with pressure, suggesting a potential preservation of PIC and POC in the sediment thanks to the sinking of aggregates.

Several studies have even shown a loss of calcite after zooplankton gut passage, which contrasts with the observation of well-preserved coccoliths within zooplankton fecal pellets (Harris, 1994; Honjo, 1976; Honjo and Roman, 1978; Roth et al., 1975; Samtleben and Bickert, 1990). Indeed, numerical models using a timeframe and pH inside copepod guts suggest a moderate calcite dissolution inside the gut (Jansen and Wolf-Gladrow, 2001). Langer et al. (2007) observed that calcite dissolution during copepod gut passage was below 8% of the weight of the coccoliths of *Calcidiscus leptoporus* inside fecal pellets, but these coccoliths were intact and showed no evidence of any dissolution. In addition, Antia et al. (2008) successfully observed that coccolith dissolution/fragmentation occurs inside microzooplankton vacuoles (also recently observed by Dean et al., 2024), but not after copepod guts passage (also described in Toullec et al., 2022).

4.4.2. The biogeographical pattern of zooplankton-mediated dissolution

Two experimental studies demonstrated that microzooplankton vacuole induce PIC dissolution (Antia et al., 2008: Dean et al., 2024). Microzooplankton (< 200 µm, dominated by protists) regulate primary producer biomass and particulate organic carbon transfer through the food web, where a fraction could then be exported as fecal pellet or aggregates (McNair et al., 2021). The contributions of microzooplankton grazing to the ocean's biological carbon remineralization are considered as the same magnitude as bacterial respiration (Calbet and Landry, 2004). However, ecosystemic differences in microzooplankton grazing/particle export flux or trophic structure have been largely underestimated within biogeochemical models that seek to predict the microbial community's role in the oceanic carbon flux.

The percentage of annual primary production grazed by microzooplankton increases with temperature, such as in open oceans, microzooplankton consumption varies from 59% for temperate–subpolar and polar systems to 75% for tropical–subtropical regions (Calbet and Landry, 2004). Annual higher grazing rates by microzooplankton are also expected in sub-tropical regions due to no seasonal bias, leading to continuous grazing pressure from microzooplankton. At the end of the North Atlantic phytoplankton blooms, microzooplankton consume the equivalent of 100–800% of their body carbon each day, which is more than an order of magnitude higher than copepods. Microzooplankton in the mixed layer grazed between 288 and 589 mg C m^{-2} day^{-1} and accounted for between 39 and 115% of the phytoplankton production In the North-Eastern Atlantic during mid-summer (Burkill et al., 1993).

4.4.3. PIC production timing of and flux pathway

4.4.3.1. Zooplankton impact on PIC dissolution and/or conservation

Irigoien et al. (2005) hypothesized that blooming species are capable of escaping control by microzooplankton grazing through a combination of predation avoidance mechanisms (e.g. colonies, larger size, spines, and toxic compounds) at the beginning of the bloom (Irigoien et al., 2005). In a temperate ecosystem, where the season variability is a determinant for PIC export flux (see Fig. 6), the coccolithophore blooms, by the large abundance of $CaCO_3$ coccoliths could be also considered as a predation avoidance mechanism (Monteiro et al., 2016). By this way, blooming coccolithophores such as *Emiliania huxleyi* could produce too much biomass that microzooplankton grazing pressure won't be significantly sufficient to dissolve the $CaCO_3$ coccoliths in their acid vacuole. On the opposite, in subtropics and equatorial ecosystems, the annual constant coccolithophore biomass (low seasonal bias, see Fig. 6) regarding the annual consistent microzooplankton grazing pressure, coccoliths may not constitute a sufficient predation avoidance mechanism, and so could be continuously dissolved inside microzooplankton acid vacuole (Antia et al., 2008, Dean et al., 2024). Coccolithophore blooming conditions could indeed interfere with predator-prey control, permitting massive particle sinking flux thanks to aggregation formation and repackaging by mesozooplankton (e.g.: copepods and larvaceans). Moreover, large zooplankton (e.g. *Calanus* spp.) graze on microzooplankton, which could significantly reduce the microzooplankton community biomass. Indeed, the mesocosm experiment demonstrated that large copepod (*Calanus finmarchicus*) ingestion rates were similar during blooms of diatoms and E. *huxleyi* (Nejstgaard et al., 1994). However, C. *finmarchicus* biomass increased 3 times more in mesocosms dominated by E. *huxleyi* compared to mesocosms with diatom blooms at similar algal biomass (Nejstgaard et al., 1994). The authors suggested that during bloom conditions, copepods "preferentially" graze on the microzooplankton (Nejstgaard et al., 1994). The incorporation of coccoliths inside large fecal pellets (mesozooplankton) is the result of passive non-selective feeding behaviour (e.g. current feeding, see detail below), and not necessarily selective grazing on coccolithophores.

Our dataset demonstrated that in the North Atlantic (NA), the linear regression slope between PIC production and PIC flux at different layers of depth is positive, meaning that the more PIC is produced, the more PIC flux is (Fig. 5). This positive relation is observed at every layer of depth considered in this study. During North Atlantic phytoplankton bloom phenology, grazing by microzooplankton increased when the bloom declined (typically at the end of June; Grifford et al., 1995). Microzooplankton consume up to 100% of potential daily chlorophyll *a* production at the end of the bloom (Gifford et al., 1995).

This study demonstrates a stronger correlation between NPP and PIC flux compared to PIC production and PIC flux (Fig. 4). At the global scale, a positive relationship between average net primary production and zooplankton biomass is observed in the epi-, meso-, and bathypelagic layers (Hernández-León et al., 2020). Moreover, the study of Hernández-León et al. (2020) suggests that this relationship could enhance the organic carbon transfer to the deep ocean (fecal pellet and excretion) and deep remineralization supported by an active carbon transport process associated with vertical zooplankton migration.

4.4.3.2. Zooplankton functional groups and dissolution pattern

A recent work based on global zooplankton data set and habitat modelling suggests that distinct copepod functional traits (e.g.: body size, feeding behaviour) are associated with different bioregions (Benedetti et al., 2023). In this study, the authors described temperate and sub-polar regions dominated by large copepods, represented by detritivores/omnivorous species and associated with passive feeding modes (current-feeders or cruise-feeders, Fig. 5 in Benedetti et al., 2023). On the other hand, subtropics and equatorial upwelling are dominated by smaller copepods (2 – 2.5 mm), represented by carnivorous species and preferentially associated with active feeding modes (ambush-feeders and current-ambush-feeders, see Fig. 5 in Benedetti et al., 2023). Several studies showed grazing characteristics associated with zooplankton functional groups induce a control on the biomass and diversity of other functional groups and phytoplankton biomass as well, with consequences for global biogeochemical cycles (Le Quéré et al., 2016; Vallina et al., 2014). This study hypothesises that zooplankton functional groups could control the PIC export efficiency and transfer efficiency, probably mediated by guts and vacuoles dissolution of $CaCO_3$. A summary of the hypothetic mechanism is displayed in Fig. 7. In temperate areas, large copepods (e.g. *Calanus* spp.) could apply strong grazing pressure on microzooplankton (Nejstgaard et al., 1997, 1994), which could induce a trophic cascade

(Wassmann, 1998). Indeed, it has been demonstrated that high trophic levels indirectly affect microbial ecosystems (Leising et al., 2005; Zöllner et al., 2009). The present study suggests that in temperate and subpolar ecosystems, large copepods could increase the PIC export flux efficiency in 2 different ways: 1) Repackage coccoliths into fecal pellet (passive current feeding). 2) Apply a strong enough grazing pressure on microzooplankton, which could indirectly reduce $CaCO_3$-mediated dissolution by microzooplankton (Dean et al., 2024).

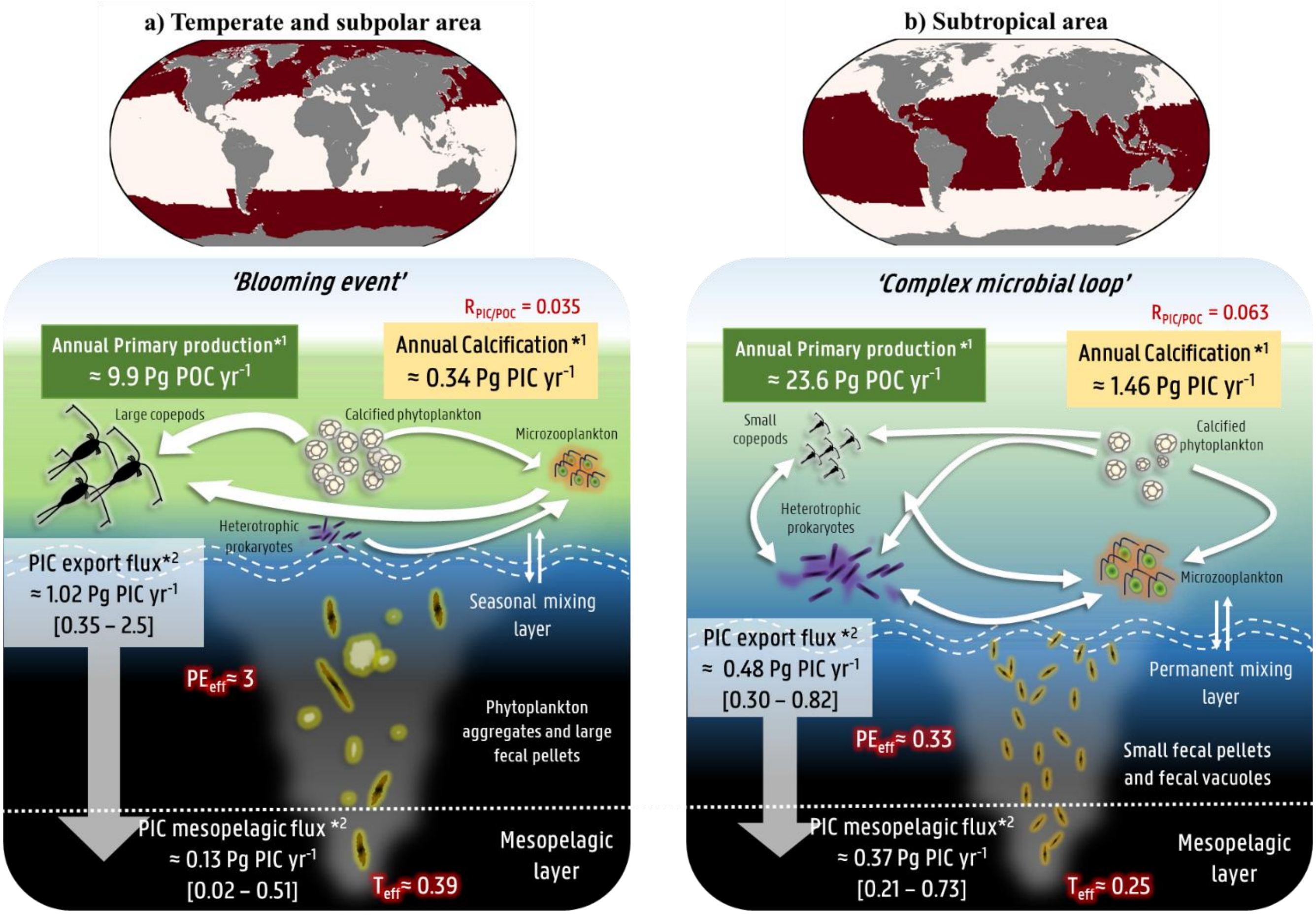

*1 Satellite based NPP, excluding continental margin (200m depth) and interior sea

*2 Estimates based on the sediment trap annual PIC flux (g C m^{-2} yr^{-1}) extended to the total surface area. Results are expressed by the median and interquartile [q25 – q75]

Figure 7: Synthesis of the potential PIC pathway through the water column, in two distinct ecosystems: a) Subtropical ecosystems (subtropical gyres and equatorial upwellings). b) Temperate zone (North Atlantic, North Pacific and subpolar regions). The white arrows represent the trophic transfer between the different planktonic compartments (Predator prey), double arrow means that both compartments could be both prey and predator each other. Small copepods correspond to individual body sizes ranging from 200 µm to 2 mm; Microzooplankton (mostly protists, < 200 µm) represent the flagellates and ciliates community; Large copepods correspond to individual body sizes larger than 2 mm (mostly large calanoid). Note that microzooplankton could be heterotrophic, autotrophic or mixotrophic.

5. Conclusion and perspectives

In this study, the ‘packaging factor’ theory is suggested to be an important driver of the discrepancy between the estimated PIC production and the export flux in distinct oceanic regions. Despite the PIC/POC production ratio being twice as high in subtropical areas compared to temperate and subpolar areas, the PE_{eff} is estimated 10 times lower and the T_{eff} 1.5 times lower. This study suggests that the zooplankton functional diversity and biogeography could explain the different patterns of $CaCO_3$ export efficiency, considering different patterns of dissolution and conservation into particles. Such a process could significantly contribute to the total downward export of carbon and associated nutrients. However, only few experimental studies have demonstrated the actual effect of zooplankton functional diversity effect on $CaCO_3$ dissolution. To confirm and complete this present study hypothesis, there is a strong need for experimental data and *in situ* observations regarding both mesozooplankton and microzooplankton grazing dynamic and $CaCO_3$ flux. In a context of surface ocean warming and acidification, phytoplankton losses due to microzooplankton grazing in eutrophic waters are expected to increase (Chen et al., 2012), which could have an attenuation effect on carbonate pumps within temperate regions. In addition, POC export will not respond equally across all high-latitude regions to possible future changes in ballast availability, which could also have consequences in the BCP. Data compilation and model output demonstrated that coccolithophores generally tend to be less calcified relatively to growth when the CO_2 increases (Krumhardt et al., 2017, 2019). The end-of-century CO_2 concentrations projection result 11% less oceanic calcification on a global scale relative to preindustrial CO_2 levels (Krumhardt et al., 2019). All this implication in surface ocean dynamics would have consequences on future surface alkalinity balance and CO_2 exchange between ocean and atmosphere (Planchat et al., 2024; Tyrrell, 2008; Volk & Hoffert, 1985).

Code and Data availability. The author confirms that the data supporting the findings of this study are available within the article and its Supplement.

Author’s contribution. Jordan Toullec: Conceptualization, Data curation, Formal analysis, Investigation, Methodology, Validation, Visualization, Writing original draft, study and editing.

Competing interest. The author declare that they have no known competing financial interests or personal relationships that could have appeared to influence the work reported in this paper.

Financial support. Jordan Toullec worked on this study while he was a post-doctorate fellow funded by CARBOCEAN ERC project: ERC-StG2019-853516. Jordan Toullec is now a post-doctorate fellow funded by CLIMArcTIC PPR project : *‘Océan et Climat’ Défi 2: Intensifier les recherches dans des océans polaires en pleine mutation et aux enjeux géostratégiques majeurs.*

6. References

Antia, A. N., Suffrian, K., Holste, L., Müller, M. N., Nejstgaard, J. C., Simonelli, P., Carotenuto, Y., and Putzeys, S.: Dissolution of coccolithophorid calcite by microzooplankton and copepod grazing, Biogeosciences discussion, https://doi.org/10.5194/bgd-5-1-2008, 2008.

Antoine, D. and Morel, A.: Oceanic primary production: 1. Adaptation of a spectral light-photosynthesis model in view of application to satellite chlorophyll observations, Global Biogeochemical Cycles, 10, 43–55, https://doi.org/10.1029/95GB02831, 1996.

Balch, W. M. and Mitchell, C.: Remote sensing algorithms for particulate inorganic carbon (PIC) and the global cycle of PIC, Earth-Science Reviews, 239, 104363, https://doi.org/10.1016/j.earscirev.2023.104363, 2023.

Balch, W. M., Kilpatrick, K. A., Holligan, P., Harbour, D., and Fernandez, E.: The 1991 coccolithophore bloom in the central North Atlantic. 2. Relating optics to coccolith concentration, Limnology and Oceanography, 41, 1684–1696, https://doi.org/10.4319/lo.1996.41.8.1684, 1996.

Balch, W. M., Gordon, H. R., Bowler, B. C., Drapeau, D. T., and Booth, E. S.: Calcium carbonate measurements in the surface global ocean based on Moderate-Resolution Imaging Spectroradiometer data, Journal of Geophysical Research: Oceans, 110, https://doi.org/10.1029/2004JC002560, 2005.

Balch, W. M., Drapeau, D. T., Bowler, B. C., Lyczskowski, E., Booth, E. S., and Alley, D.: The contribution of coccolithophores to the optical and inorganic carbon budgets during the Southern Ocean Gas Exchange Experiment: New evidence in support of the "Great Calcite Belt" hypothesis, Journal of Geophysical Research: Oceans, 116, https://doi.org/10.1029/2011JC006941, 2011.

Balch, W. M., Bowler, B. C., Drapeau, D. T., Lubelczyk, L. C., and Lyczkowski, E.: Vertical Distributions of Coccolithophores, PIC, POC, Biogenic Silica, and Chlorophyll a Throughout the Global Ocean, Global Biogeochemical Cycles, 32, 2–17, https://doi.org/10.1002/2016GB005614, 2018.

Barton, A. D., Pershing, A. J., Litchman, E., Record, N. R., Edwards, K. F., Finkel, Z. V., Kiørboe, T., and Ward, B. A.: The biogeography of marine plankton traits, Ecology Letters, 16, 522–534, https://doi.org/10.1111/ele.12063, 2013.

Bednaršek, N., Možina, J., Vogt, M., O'Brien, C., and Tarling, G. A.: The global distribution of pteropods and their contribution to carbonate and carbon biomass in the modern ocean, Earth System Science Data, 4, 167–186, https://doi.org/10.5194/essd-4-167-2012, 2012.

Benedetti, F., Wydler, J., and Vogt, M.: Copepod functional traits and groups show divergent biogeographies in the global ocean, Journal of Biogeography, 50, 8–22, https://doi.org/10.1111/jbi.14512, 2023.

Berelson, W. M., Balch, W. M., Najjar, R., Feely, R. A., Sabine, C., and Lee, K.: Relating estimates of CaCO3 production, export, and dissolution in the water column to measurements of CaCO3 rain into sediment traps and dissolution on the sea floor: A revised global carbonate budget, Global Biogeochemical Cycles, 21, https://doi.org/10.1029/2006GB002803, 2007.

Berner, R. A. and Morse, J. W.: Dissolution kinetics of calcium carbonate in sea water; IV, Theory of calcite dissolution, American Journal of Science, 274, 108–134, https://doi.org/10.2475/ajs.274.2.108, 1974.

Bissett, A., Neu, T. R., and Beer, D. de: Dissolution of Calcite in the Twilight Zone: Bacterial Control of Dissolution of Sinking Planktonic Carbonates Is Unlikely, PLOS ONE, 6, e26404, https://doi.org/10.1371/journal.pone.0026404, 2011.

Brandão, S. N., Hoppema, M., Kamenev, G. M., Karanovic, I., Riehl, T., Tanaka, H., Vital, H., Yoo, H., and Brandt, A.: Review of Ostracoda (Crustacea) living below the Carbonate Compensation Depth and the deepest record of a calcified ostracod, Progress in Oceanography, 178, 102144, https://doi.org/10.1016/j.pocean.2019.102144, 2019.

Buitenhuis, E. T., Le Quéré, C., Bednaršek, N., and Schiebel, R.: Large Contribution of Pteropods to Shallow CaCO3 Export, Global Biogeochemical Cycles, 33, 458–468, https://doi.org/10.1029/2018GB006110, 2019.

Burkill, P. H., Edwards, E. S., John, A. W. G., and Sleigh, M. A.: Microzooplankton and their herbivorous activity in the northeastern Atlantic Ocean, Deep Sea Research Part II: Topical Studies in Oceanography, 40, 479–493, https://doi.org/10.1016/0967-0645(93)90028-L, 1993.

Burridge, A. K., Goetze, E., Wall-Palmer, D., Le Double, S. L., Huisman, J., and Peijnenburg, K. T. C. A.: Diversity and abundance of pteropods and heteropods along a latitudinal gradient across the Atlantic Ocean, Progress in Oceanography, 158, 213–223, https://doi.org/10.1016/j.pocean.2016.10.001, 2017.

Calbet, A. and Landry, M. R.: Phytoplankton growth, microzooplankton grazing, and carbon cycling in marine systems, Limnology and Oceanography, 49, 51–57, https://doi.org/10.4319/lo.2004.49.1.0051, 2004.

Chaabane, S., de Garidel-Thoron, T., Meilland, J., Sulpis, O., Chalk, T. B., Brummer, G. J. A., ... & Schiebel, R.: Migrating is not enough for modern planktonic foraminifera in a changing ocean. Nature, 1-7. https://doi.org /s41586-024-08191-5, 2024.

Chen, B., Landry, M. R., Huang, B., and Liu, H.: Does warming enhance the effect of microzooplankton grazing on marine phytoplankton in the ocean?, Limnology and Oceanography, 57, 519–526, https://doi.org/10.4319/lo.2012.57.2.0519, 2012.

Clements, D. J., Yang, S., Weber, T., McDonnell, A. M. P., Kiko, R., Stemmann, L., and Bianchi, D.: New Estimate of Organic Carbon Export From Optical Measurements Reveals the Role of Particle Size Distribution and Export Horizon, Global Biogeochemical Cycles, 37, e2022GB007633, https://doi.org/10.1029/2022GB007633, 2023.

Dean, C. L., Harvey, E. L., Johnson, M. D., & Subhas, A. V. Microzooplankton grazing on the coccolithophore Emiliania huxleyi and its role in the global calcium carbonate cycle. Science Advances, 10(45), eadr5453. 2024

Feely, R. A., Sabine, C. L., Lee, K., Millero, F. J., Lamb, M. F., Greeley, D., ... & Wong, C. S. In situ calcium carbonate dissolution in the Pacific Ocean. Global Biogeochemical Cycles, 16(4), 91-1. 2002.

Fischer, G., Karstensen, J., Romero, O., Baumann, K.-H., Donner, B., Hefter, J., Mollenhauer, G., Iversen, M., Fiedler, B., Monteiro, I., and Körtzinger, A.: Bathypelagic particle flux signatures from a suboxic eddy in the oligotrophic tropical North Atlantic: production, sedimentation and preservation, Biogeosciences, 13, 3203–3223, https://doi.org/10.5194/bg-13-3203-2016, 2016.

Francois, R., Honjo, S., Krishfield, R., and Manganini, S.: Factors controlling the flux of organic carbon to the bathypelagic zone of the ocean, Global Biogeochemical Cycles, 16, 34-1-34–20, https://doi.org/10.1029/2001GB001722, 2002.

Gangstø, R., Gehlen, M., Schneider, B., Bopp, L., Aumont, O., and Joos, F.: Modeling the marine aragonite cycle: changes under rising carbon dioxide and its role in shallow water $CaCO_3$ dissolution, Biogeosciences, 5, 1057–1072, https://doi.org/10.5194/bg-5-1057-2008, 2008.

Gifford, D. J., Fessenden, L. M., Garrahan, P. R., and Martin, E.: Grazing by microzooplankton and mesozooplankton in the high-latitude North Atlantic Ocean: Spring versus summer dynamics, Journal of Geophysical Research: Oceans, 100, 6665–6675, https://doi.org/10.1029/94JC00983, 1995.

Harris, R. P.: Zooplankton grazing on the coccolithophore Emiliania huxleyi and its role in inorganic carbon flux, Marine Bioliogy, 119, 431–439, https://doi.org/10.1007/BF00347540, 1994.

Hauck, J., Gruber, N., Ishii, M., and Müller, J. D.: Constraining regional and global ocean carbon fluxes in RECCAP2, Copernicus Meetings, https://doi.org/10.5194/egusphere-egu23-12786, 2023.

Henson, S. A., Sanders, R., and Madsen, E.: Global patterns in efficiency of particulate organic carbon export and transfer to the deep ocean: EXPORT AND TRANSFER EFFICIENCY, Global Biogeochem. Cycles, 26, n/a-n/a, https://doi.org/10.1029/2011GB004099, 2012.

Hernández-León, S., Koppelmann, R., Fraile-Nuez, E., Bode, A., Mompeán, C., Irigoien, X., Olivar, M. P., Echevarría, F., Fernández de Puelles, M. L., González-Gordillo, J. I., Cózar, A., Acuña, J. L., Agustí, S., and Duarte, C. M.: Large deep-sea zooplankton biomass mirrors primary production in the global ocean, Nat Commun, 11, 6048, https://doi.org/10.1038/s41467-020-19875-7, 2020.

Holligan, P. M., Fernández, E., Aiken, J., Balch, W. M., Boyd, P., Burkill, P. H., Finch, M., Groom, S. B., Malin, G., Muller, K., Purdie, D. A., Robinson, C., Trees, C. C., Turner, S. M., and van der Wal, P.: A biogeochemical study of the coccolithophore, Emiliania huxleyi, in the North Atlantic, Global Biogeochemical Cycles, 7, 879–900, https://doi.org/10.1029/93GB01731, 1993.

Honjo, S.: Coccoliths: Production, transportation and sedimentation, Marine Micropaleontology, 1, 65–79, https://doi.org/10.1016/0377-8398(76)90005-0, 1976.

Honjo, S. and Roman, M.: Marine copepod fecal pellets: Production, preservation and sedimentation, Journal of Marine Research, 36, 1978.

Hopkins, J. and Balch, W. M.: A New Approach to Estimating Coccolithophore Calcification Rates From Space, Journal of Geophysical Research: Biogeosciences, 123, 1447–1459, https://doi.org/10.1002/2017JG004235, 2018.

Irigoien, X., Flynn, K. J., and Harris, R. P.: Phytoplankton blooms: a ‘loophole’ in microzooplankton grazing impact?, Journal of Plankton Research, 27, 313–321, https://doi.org/10.1093/plankt/fbi011, 2005.

Iversen, M. H. and Ploug, H.: Ballast minerals and the sinking carbon flux in the ocean: carbon-specific respiration rates and sinking velocity of marine snow aggregates, Biogeosciences, 7, 2613–2624, https://doi.org/10.5194/bg-7-2613-2010, 2010.

Jansen, H. and Wolf-Gladrow, D.: Carbonate dissolution in copepod guts: a numerical model, Mar. Ecol. Prog. Ser., 221, 199–207, https://doi.org/10.3354/meps221199, 2001.

Kaneko, H., Endo, H., Henry, N., Berney, C., Mahé, F., Poulain, J., Labadie, K., Beluche, O., El Hourany, R., Chaffron, S., Wincker, P., Nakamura, R., Karp-Boss, L., Boss, E., Chris Bowler, de Vargas, C., Tomii, K., and Ogata, H.: Predicting global distributions of eukaryotic plankton communities from satellite data, ISME COMMUN., 3, 1–9, https://doi.org/10.1038/s43705-023-00308-7, 2023.

Klaas, C. and Archer, D. E.: Association of sinking organic matter with various types of mineral ballast in the deep sea: Implications for the rain ratio, Global Biogeochemical Cycles, 16, 63-1-63–14, https://doi.org/10.1029/2001GB001765, 2002.

Knecht, N. S., Benedetti, F., Elizondo, U. H., Bednaršek, N., Chaabane, S., de Weerd, C., Peijnenburg, K. T. C. A., Schiebel, R., and Vogt, M.: The impact of zooplankton calcifiers on the marine carbon cycle, Global Biogeochemical Cycles, n/a, e2022GB007685, https://doi.org/10.1029/2022GB007685, 2023.

Krumhardt, K. M., Lovenduski, N. S., Iglesias-Rodriguez, M. D., and Kleypas, J. A.: Coccolithophore growth and calcification in a changing ocean, Progress in Oceanography, 159, 276–295, https://doi.org/10.1016/j.pocean.2017.10.007, 2017.

Krumhardt, K. M., Lovenduski, N. S., Long, M. C., Lévy, M., Lindsay, K., Moore, J. K., & Nissen, C. Coccolithophore growth and calcification in an acidified ocean: Insights from community Earth system model simulations. Journal of Advances in Modeling Earth Systems, 11(5), 1418-1437. 2019

Kwon, E. Y., Dunne, J. P., & Lee, K. Biological export production controls upper ocean calcium carbonate dissolution and CO2 buffer capacity. Science Advances, 10(13), eadl0779. 2024

Langer, G., Nehrke, G., and Jansen, S.: Dissolution of Calcidiscus leptoporus coccoliths in copepod guts? A morphological study, Mar. Ecol. Prog. Ser., 331, 139–146, https://doi.org/10.3354/meps331139, 2007.

Laurenceau-Cornec, E. C., Le Moigne, F. A. C., Gallinari, M., Moriceau, B., Toullec, J., Iversen, M. H., Engel, A., and De La Rocha, C. L.: New guidelines for the application of Stokes' models to the sinking velocity of marine aggregates, Limnology and Oceanography, 65, 1264–1285, https://doi.org/10.1002/lno.11388, 2020.

Le Moigne, F. A. C., Pabortsava, K., Marcinko, C. L. J., Martin, P., and Sanders, R. J.: Where is mineral ballast important for surface export of particulate organic carbon in the ocean?, Geophysical Research Letters, 41, 8460–8468, https://doi.org/10.1002/2014GL061678, 2014.

Le Quéré, C., Buitenhuis, E. T., Moriarty, R., Alvain, S., Aumont, O., Bopp, L., Chollet, S., Enright, C., Franklin, D. J., Geider, R. J., Harrison, S. P., Hirst, A. G., Larsen, S., Legendre, L., Platt, T., Prentice, I. C., Rivkin, R. B., Sailley, S., Sathyendranath, S., Stephens, N., Vogt, M., and Vallina, S. M.: Role of zooplankton dynamics for Southern Ocean phytoplankton biomass and global biogeochemical cycles, Biogeosciences, 13, 4111–4133, https://doi.org/10.5194/bg-13-4111-2016, 2016.

Lebrato, M., Iglesias-Rodríguez, D., Feely, R. A., Greeley, D., Jones, D. O. B., Suarez-Bosche, N., Lampitt, R. S., Cartes, J. E., Green, D. R. H., and Alker, B.: Global contribution of echinoderms to the marine carbon cycle: CaCO3 budget and benthic compartments, Ecological Monographs, 80, 441–467, https://doi.org/10.1890/09-0553.1, 2010.

Lee, K.: Global net community production estimated from the annual cycle of surface water total dissolved inorganic carbon, Limnology and Oceanography, 46, 1287–1297, https://doi.org/10.4319/lo.2001.46.6.1287, 2001.

Leising, A. W., Pierson, J. J., Halsband-Lenk, C., Horner, R., and Postel, J.: Copepod grazing during spring blooms: Can Pseudocalanus newmani induce trophic cascades?, Progress in Oceanography, 67, 406–421, https://doi.org/10.1016/j.pocean.2005.09.009, 2005.

Lima, I. D., Lam, P. J., and Doney, S. C.: Dynamics of particulate organic carbon flux in a global ocean model, Biogeosciences, 11, 1177–1198, https://doi.org/10.5194/bg-11-1177-2014, 2014.

Milliman, J. D., Troy, P. J., Balch, W. M., Adams, A. K., Li, Y.-H., and Mackenzie, F. T.: Biologically mediated dissolution of calcium carbonate above the chemical lysocline?, Deep Sea Research Part I: Oceanographic Research Papers, 46, 1653–1669, https://doi.org/10.1016/S0967-0637(99)00034-5, 1999.

Monteiro, F. M., Bach, L. T., Brownlee, C., Bown, P., Rickaby, R. E. M., Poulton, A. J., Tyrrell, T., Beaufort, L., Dutkiewicz, S., Gibbs, S., Gutowska, M. A., Lee, R., Riebesell, U., Young, J., and Ridgwell, A.: Why marine phytoplankton calcify, Sci. Adv., 2, e1501822, https://doi.org/10.1126/sciadv.1501822, 2016.

Mouw, C. B., Barnett, A., McKinley, G. A., Gloege, L., and Pilcher, D.: Global ocean particulate organic carbon flux merged with satellite parameters, Earth System Science Data, 8, 531–541, https://doi.org/10.5194/essd-8-531-2016, 2016.

Nejstgaard, J., Gismervik, I., and Solberg, P.: Feeding and reproduction by Calanus finmarchicus, and microzooplankton grazing during mesocosm blooms of diatoms and the coccolithophore Emiliania huxleyi, Mar. Ecol. Prog. Ser., 147, 197–217, https://doi.org/10.3354/meps147197, 1997.

Nejstgaard, J. C., Witte, H. J., van der Wal, P., and Jacobsen, A.: Copepod grazing during a mesocosm study of an Emiliania huxleyi (Prymnesiophyceae) bloom, Sarsia, 79, 369–377, https://doi.org/10.1080/00364827.1994.10413568, 1994.

Neukermans, G., Bach, L. T., Butterley, A., Sun, Q., Claustre, H., and Fournier, G. R.: Quantitative and mechanistic understanding of the open ocean carbonate pump - perspectives for remote sensing and autonomous in situ observation, Earth-Science Reviews, 104359, https://doi.org/10.1016/j.earscirev.2023.104359, 2023.

Nowicki, M., DeVries, T., and Siegel, D. A.: Quantifying the Carbon Export and Sequestration Pathways of the Ocean's Biological Carbon Pump, Global Biogeochemical Cycles, 36, e2021GB007083, https://doi.org/10.1029/2021GB007083, 2022.

Passow, U. and Carlson, C.: The biological pump in a high CO2 world, Mar. Ecol. Prog. Ser., 470, 249–271, https://doi.org/10.3354/meps09985, 2012.

Pilskaln, C. H. and Honjo, S.: The Fecal Pellet fraction of biogeochemical particle fluxes to the deep sea, Global Biogeochem. Cycles, 1, 31–48, https://doi.org/10.1029/GB001i001p00031, 1987.

Planchat, A., Kwiatkowski, L., Bopp, L., Torres, O., Christian, J. R., Butenschön, M., ... & Stock, C. The representation of alkalinity and the carbonate pump from CMIP5 to CMIP6 Earth system models and implications for the carbon cycle. Biogeosciences, 20(7), 1195-1257. 2023

Planchat, A., Bopp, L., Kwiatkowski, L., & Torres, O. The carbonate pump feedback on alkalinity and the carbon cycle in the 21st century and beyond. Earth System Dynamics, 15(3), 565-588. 2024

Ricour, F., Guidi, L., Gehlen, M., DeVries, T., and Legendre, L.: Century-scale carbon sequestration flux throughout the ocean by the biological pump, Nat. Geosci., 1–9, https://doi.org/10.1038/s41561-023-01318-9, 2023.

Romero, O. E., Fischer, G., Karstensen, J., and Cermeño, P.: Eddies as trigger for diatom productivity in the open-ocean Northeast Atlantic, Progress in Oceanography, 147, 38–48, https://doi.org/10.1016/j.pocean.2016.07.011, 2016.

Rosengard, S. Z., Lam, P. J., Balch, W. M., Auro, M. E., Pike, S., Drapeau, D., and Bowler, B.: Carbon export and transfer to depth across the Southern Ocean Great Calcite Belt, Biogeosciences, 12, 3953–3971, https://doi.org/10.5194/bg-12-3953-2015, 2015.

Roth, P. H., Mullin, M. M., and Berger, W. H.: Coccolith Sedimentation by Fecal Pellets: Laboratory Experiments and Field Observations, Geol Soc America Bull, 86, 1079, https://doi.org/10.1130/0016-7606(1975)86<1079:CSBFPL>2.0.CO;2, 1975.

Samtleben, C. and Bickert, T.: Coccoliths in sediment traps from the Norwegian Sea, Marine Micropaleontology, 16, 39–64, https://doi.org/10.1016/0377-8398(90)90028-K, 1990.

Sarmiento, J. L.: Ocean Biogeochemical Dynamics, in: Ocean Biogeochemical Dynamics, Princeton University Press, https://doi.org/10.1515/9781400849079, 2013.

Savoye, N., Benitez-Nelson, C., Burd, A. B., Cochran, J. K., Charette, M., Buesseler, K. O., ... & Elskens, M. 234Th sorption and export models in the water column: A review. Marine Chemistry, 100(3-4), 234-249. 2006.

Schiebel, R. and Movellan, A.: First-order estimate of the planktic foraminifer biomass in the modern ocean, Earth System Science Data, 4, 75–89, https://doi.org/10.5194/essd-4-75-2012, 2012.

Sulpis, O., Jeansson, E., Dinauer, A., Lauvset, S. K., and Middelburg, J. J.: Calcium carbonate dissolution patterns in the ocean, Nat. Geosci., 14, 423–428, https://doi.org/10.1038/s41561-021-00743-y, 2021.

https://doi.org/10.5194/egusphere-2025-1108
Preprint. Discussion started: 22 April 2025

Tamburini, C., Garel, M., Barani, A., Boeuf, D., Bonin, P., Bhairy, N., Guasco, S., Jacquet, S., Le Moigne, F. A. C., Panagiotopoulos, C., Riou, V., Veloso, S., Santinelli, C., and Armougom, F.: Increasing Hydrostatic Pressure Impacts the Prokaryotic Diversity during Emiliania huxleyi Aggregates Degradation, Water, 13, 2616, https://doi.org/10.3390/w13192616, 2021.

Thuiller, W., Pollock, L. J., Gueguen, M., and Münkemüller, T.: From species distributions to meta-communities, Ecology Letters, 18, 1321–1328, https://doi.org/10.1111/ele.12526, 2015.

Torres Valdés, S., Painter, S. C., Martin, A. P., Sanders, R., and Felden, J.: Data compilation of fluxes of sedimenting material from sediment traps in the Atlantic Ocean, Earth System Science Data, 6, 123–145, https://doi.org/10.5194/essd-6-123-2014, 2014.

Toullec, J., Vincent, D., Frohn, L., Miner, P., Le Goff, M., Devesa, J., and Moriceau, B.: Copepod Grazing Influences Diatom Aggregation and Particle Dynamics, Frontiers in Marine Science, 6, https://doi.org/10.3389/fmars.2019.00751, 2019.

Toullec, J., Delegrange, A., Perruchon, A., Duong, G., Cornille, V., Brutier, L., and Hermoso, M.: Copepod Feeding Responses to Changes in Coccolithophore Size and Carbon Content, Journal of Marine Science and Engineering, 10, 1807, https://doi.org/10.3390/jmse10121807, 2022.

Tyrrell, T. and Merico, A.: Emiliania huxleyi: bloom observations and the conditions that induce them, in: Coccolithophores: From Molecular Processes to Global Impact, edited by: Thierstein, H. R. and Young, J. R., Springer, Berlin, Heidelberg, 75–97, https://doi.org/10.1007/978-3-662-06278-4_4, 2004.

Tyrrell, T. Calcium carbonate cycling in future oceans and its influence on future climates. Journal of plankton research, 30(2), 141-156. 2008.

Vallina, S. M., Follows, M. J., Dutkiewicz, S., Montoya, J. M., Cermeno, P., and Loreau, M.: Global relationship between phytoplankton diversity and productivity in the ocean, Nat Commun, 5, 4299, https://doi.org/10.1038/ncomms5299, 2014.

Volk, T., & Hoffert, M. I. Ocean carbon pumps: Analysis of relative strengths and efficiencies in ocean-driven atmospheric CO2 changes. The carbon cycle and atmospheric CO2: Natural variations Archean to present, 32, 99-110. 1985

Wang, W.-L., Fu, W., Le Moigne, F. A. C., Letscher, R. T., Liu, Y., Tang, J.-M., and Primeau, F. W.: Biological carbon pump estimate based on multidecadal hydrographic data, Nature, 1–7, https://doi.org/10.1038/s41586-023-06772-4, 2023.

Wassmann, P.: Retention versus export food chains: processes controlling sinking loss from marine pelagic systems, in: Eutrophication in Planktonic Ecosystems: Food Web Dynamics and Elemental Cycling: Proceedings of the Fourth International PELAG Symposium, held in Helsinki, Finland, 26–30 August 1996, edited by: Tamminen, T. and Kuosa, H., Springer Netherlands, Dordrecht, 29–57, https://doi.org/10.1007/978-94-017-1493-8_3, 1998.

Ziveri, P., Gray, W. R., Anglada-Ortiz, G., Manno, C., Grelaud, M., Incarbona, A., Rae, J. W. B., Subhas, A. V., Pallacks, S., White, A., Adkins, J. F., and Berelson, W.: Pelagic calcium carbonate production and shallow dissolution in the North Pacific Ocean, Nat Commun, 14, 1–14, https://doi.org/10.1038/s41467-023-36177-w, 2023.

Zöllner, E., Hoppe, H.-G., Sommer, U., and Jürgens, K.: Effect of zooplankton-mediated trophic cascades on marine microbial food web components (bacteria, nanoflagellates, ciliates), Limnology and Oceanography, 54, 262–275, https://doi.org/10.4319/lo.2009.54.1.0262, 2009.